



Universiteit
Leiden
The Netherlands

Kinetics of the reduction of wilt-type and mutant cytochrome c-550 by methylamin dehydrogenase and amicyanin from thiobacillus-versutus

Ubbink, M.; Hunt, N.I.; Hill, H.A.O.; Canters, G.W.

Citation

Ubbink, M., Hunt, N. I., Hill, H. A. O., & Canters, G. W. (1994). Kinetics of the reduction of wilt-type and mutant cytochrome c-550 by methylamin dehydrogenase and amicyanin from thiobacillus-versutus. *European Journal Of Biochemistry*, 222(2), 561-571.

doi:10.1111/j.1432-1033.1994.tb18898.x

Version: Publisher's Version

License: [Licensed under Article 25fa Copyright Act/Law \(Amendment Taverne\)](#)

Downloaded from: <https://hdl.handle.net/1887/3608139>

Note: To cite this publication please use the final published version (if applicable).

Kinetics of the reduction of wild-type and mutant cytochrome *c*-550 by methylamine dehydrogenase and amicyanin from *Thiobacillus versutus*

Marcellus UBBINK¹, Nick I. HUNT², H. Allen O. HILL² and Gerard W. CANTERS¹

¹ Gorlaeus Laboratories, Leiden Institute of Chemistry, Leiden University, The Netherlands

² New Chemistry Building, Department of Chemistry, University of Oxford, England

(Received January 26, 1994) – EJB 94 0093/3

To elucidate the kinetic properties of the methylamine dehydrogenase (MADH) redox chain of *Thiobacillus versutus* the reduction of cytochrome *c*-550 by MADH and amicyanin has been studied. Under steady state conditions, the rate constants of the reactions have been determined as a function of the ionic strength, both for wild type cytochrome *c*-550 and for mutants in which the conserved residue Lys14 has been replaced as follows: Lys14→Gln (mutant [K14Q]cytochrome *c*-550) and Lys14→Glu (mutant [K14E]cytochrome *c*-550).

The second-order rate constant of the reduction of cytochrome *c*-550 by MADH shows a biphasic ionic-strength dependence. At low ionic strength the rate constant remains unchanged (wild type) or increases ([K14Q]cytochrome *c*-550) with increasing ionic strength, while at high salt concentrations the rate constant decreases monotonically as the ionic strength increases. It is suggested that conformational freedom exists in the association complex and that this is favourable for electron transfer. [K14Q]cytochrome *c*-550 and [K14E]cytochrome *c*-550 are reduced at rates 20-fold and 500-fold slower than wild-type cytochrome *c*-550 by MADH, due to a lower association constant. It is concluded that MADH possesses a negative patch with which cytochrome *c*-550 associates. Lys14 plays an important role in the formation of the reaction complex.

The midpoint potentials of wild-type and mutant cytochrome *c*-550 have been determined by using cyclic voltammetry. [K14Q]cytochrome *c*-550 and [K14E]cytochrome *c*-550 show an increase in E^0 of only 2 mV and 8 mV, respectively, compared to wild-type cytochrome *c*-550 (241 mV at pH 8.1).

[K14Q]cytochrome *c*-550 and [K14E]cytochrome *c*-550 are reduced by amicyanin at rates that are only slightly faster than for wild-type cytochrome *c*-550. The difference is partly attributable to the change in E^0 . High ionic strength results in a threefold increase in the rate in all three cases. These results indicate that charge interactions do not play a major role in the formation of the amicyanin/cytochrome *c*-550 reaction complex, suggesting an interaction at the hydrophobic patch of amicyanin.

The reduction of cytochrome *c*-550 by MADH can be inhibited by Zn²⁺-substituted amicyanin. Ag⁺-amicyanin, however, has little effect on the reduction rate. These results suggest that MADH has a much higher affinity for Cu²⁺-amicyanin (substrate) than for Cu⁺-amicyanin (product).

On the basis of these findings the roles of the components of the MADH redox chain are discussed.

The Gram-negative bacterium *Thiobacillus versutus* is capable of using methylamine as a carbon and energy source. This substrate induces the production of two periplasmic proteins, methylamine dehydrogenase (MADH) and amicyanin, which are involved in the conversion of methylamine to methanal and in the subsequent respiratory electron transfer, respectively [1, 2]. MADH catalyzes the oxidation reaction

and can reduce amicyanin [3]. It has been proposed [3] that amicyanin reduces cytochrome *c*-550, one of the soluble cytochromes found in *T. versutus* grown on methylamine. Reduced cytochrome *c*-550 can be reoxidized by a membrane-bound cytochrome *aa*₃. For other bacteria that produce MADH, similar redox chains have been suggested. For *Paracoccus denitrificans* it has been shown that amicyanin is essential for growth on methylamine [4]. Controversy still exists concerning the identity of the physiological redox partner of amicyanin in this organism [5–8]. In *Methylophilus* sp. W3A1 the presence of amicyanin cannot be demonstrated and a cytochrome *c* presumably functions as the redox partner of MADH [9]. In *Methylobacterium extorquens* AM1, MADH probably donates electrons via amicyanin to a *c*-type cytochrome (*c*_H) although direct reduction of this cytochrome by MADH also appears to be possible [10].

Correspondence to G. W. Canters, Gorlaeus Laboratories, Leiden Institute of Chemistry, Leiden University, P. O. box 9502, NL-2300-RA Leiden, The Netherlands

Fax: +31 71 274349.

Abbreviations. [K14E]cytochrome *c*-550, mutant with mutation Lys14→Glu; [K14Q]cytochrome *c*-550, mutant with mutation Lys14→Gln; MADH, methylamine dehydrogenase.

Enzyme. Methylamine dehydrogenase (EC 1.4.99.3).

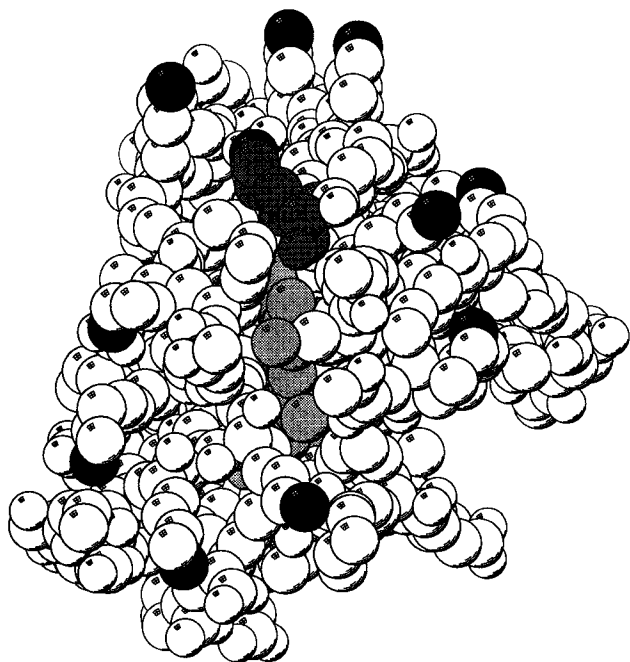


Fig. 1. Spacefilling model of cytochrome *c*-550 from *T. versutus* based on the crystal structure data of cytochrome *c*-550 from *P. denitrificans* [57]. Black spheres, N_{ϵ} of lysine residues; dark-grey spheres, Lys14; light-grey spheres, heme. The picture was produced with MOLSCRIPT [58].

MADH consists of four subunits ($\alpha_2\beta_2$) comprising two functional dimers ($\alpha\beta$) [1]. Amicyanin is a small (11.7 kDa) monomeric Cu-protein [2, 11]. Both proteins are under extensive study. The crystal structures of *T. versutus* MADH [12] and amicyanin from *P. denitrificans* [13] have been solved; the structure of the complex of *P. denitrificans* amicyanin and MADH is also established [14, 15]. Furthermore, a solution structure of amicyanin from *T. versutus* has been determined by NMR methods [16] (Kalverda, A. P., unpublished results). The β subunit of MADH contains a cofactor consisting of two covalently linked tryptophan residues with a tryptophan tryptophylquinone group [11, 17]. From genetic studies [4, 11, 18, 19, 20] it has emerged that the genes for amicyanin and MADH are part of one operon, together with other genes that may be involved in the post-translational modification of MADH. The gene for cytochrome *c*-550 is located on another part of the chromosome and is just upstream of a gene coding for a subunit of cytochrome *aa*₃ (COXI) [7, 21].

The gene encoding cytochrome *c*-550 from *T. versutus* has been expressed in *Escherichia coli* under semi-anaerobic conditions and the holo-protein can be isolated from the periplasmic space [21]. This expression system has been used to make site-specific mutants of cytochrome *c*-550. Lys14 has been mutated into an uncharged (glutamine) residue and a negatively charged (glutamate) residue [22]. This lysine residue is conserved as K13 in mitochondrial cytochrome *c*. It is located near the site where the heme penetrates the protein surface (Fig. 1) and is part of the ring of positive charges around this site. Many investigations have indicated that K13 plays a key role in the electrostatic interactions with other redox proteins [23–28], small molecules [29] and in the electron self-exchange reaction [30]. The analogous lysine residue in cytochrome *c*₂ is involved in the complex formation with cytochrome *bc*₁ [31] and the photosynthetic reac-

tion center [32]. The construction of the mutants [K14Q]cytochrome *c*-550 (Lys14→Gln) and [K14E]cytochrome *c*-550 (Lys14→Glu) has enabled the study of the importance of Lys14 in the electron self-exchange reaction of cytochrome *c*-550 [22].

In this study, the mutants are used to investigate the reactions of MADH and amicyanin with cytochrome *c*-550. While the reduction of amicyanin by MADH is fast the re-oxidation of amicyanin by cytochrome *c*-550 appears to be slow, although cytochrome *c*-550 is believed to be the redox partner of amicyanin [3]. To obtain more insight into this paradox, the steady-state kinetics of the reduction of cytochrome *c*-550 by amicyanin and by MADH have been studied with both wild-type cytochrome *c*-550, [K14Q]cytochrome *c*-550 and [K14E]cytochrome *c*-550; the rate constants have been determined as a function of the ionic strength (*I*). Also, the effects of possible complex formation of MADH and amicyanin on the reaction with cytochrome *c*-550 have been studied, using redox-inactive amicyanin substitutes. Finally, the midpoint potentials of wild-type and mutant cytochrome *c*-550 have been measured with cyclic voltammetry to enable interpretation of the kinetic results.

MATERIALS AND METHODS

Mutagenesis

The construction of mutants [K14Q]cytochrome *c*-550 and [K14E]cytochrome *c*-550 has been described elsewhere [22].

Protein expression and purification

Wild-type cytochrome *c*-550 was isolated from *T. versutus* grown on methylamine or from *E. coli* after heterologous expression. [K14Q]cytochrome *c*-550 and [K14E]cytochrome *c*-550 were expressed in *E. coli* and were subsequently isolated. Growth conditions and purification procedures have been described [21, 22]. Heterologously expressed [11] and purified *T. versutus* amicyanin was a kind gift of A. P. Kalverda.

Partially purified *T. versutus* MADH was kindly provided by F. Huitema. To remove potential traces of cytochrome *c*-550 and amicyanin, MADH was applied (65 mg/1.5 ml) to a Sephacryl S-200 gel-filtration column (2.6 cm×50 cm) and eluted with 20 mM sodium phosphate (pH 7.0), containing 200 mM NaCl. After SDS/PAGE, the purity was estimated to be 90% with no bands smaller than 20 kDa.

Preparation of apo-, Zn- and Ag-amicyanin

For the preparation of apo-amicyanin, 0.4–2 μ mol Cu(II)-amicyanin was incubated overnight in 10 ml 100 mM KCN and 150 mM Tris/HCl, pH 8, at 5°C [33]. Subsequently, the protein was concentrated and diluted extensively with 20 mM Hepes/NaOH, pH 7.5, and 1 mM EDTA in an Amicon stirred cell to remove Tris and KCN.

To obtain metal-substituted amicyanin, apo-protein was incubated for 1 h with 1 mM ZnCl₂ or AgNO₃ in 20 mM Hepes/NaOH, pH 7.5, followed by several cycles of concentration and dilution with the buffer to remove excess metal ions. Apo-amicyanin could be reconstituted with Cu(II) to > 85% according to the 280/596 nm absorption ratio. Zn-amicyanin and Ag-amicyanin could not be reconstituted with Cu(II) to any extent. On an IEF gel apo-, Zn- and Ag-amicy-

anin migrated with native amicyanin [which has the same pI for the Cu(II)-form and Cu(I)-form]. Denatured amicyanin showed a broad band at a much higher pI value.

MADH activity

Some variation in activity (*vide infra*) between MADH samples was observed. Samples were stored at -20°C for over a year with little decrease in activity. Therefore, the variation in activity is not (fully) attributable to aging. This variability may have been caused by contaminants in the buffer since the MADH concentrations used were quite low. It was observed that Tris/HCl partly inhibits MADH activity. The presence of Zn^{2+} appeared to enhance the activity. However, this was not investigated further.

The activity of the most active sample was quantified by measuring the reduction rate of Wurster's blue [1] by MADH in the presence of excess methylamine (10 mM). The concentration of MADH in this sample was determined optically using the absorbance at 440 nm of the fully oxidized MADH with $\epsilon_{440} = 21 \times 10^3 \text{ M}^{-1} \cdot \text{cm}^{-1}$ [34]. The specific activity of this sample was 455 U/ μmol . The rate at which wild-type cytochrome *c*-550 was reduced by this MADH solution was used as a secondary standard to establish the MADH concentration in the samples used in subsequent experiments.

Kinetic measurements

All measurements were performed in 20 mM Hepes/NaOH, pH 8.2, with 10 mM methylamine/HCl at $29 \pm 2^{\circ}\text{C}$. KCl was added to adjust the ionic strength (*I*). *I* values include the contributions of Hepes/NaOH and methylamine/HCl (*I* = 27 mM). The total sample volume was 2.5 ml. Subsequently, concentrated solutions with known concentrations of MADH, methylamine, and amicyanin (if required) were added; the added amounts were determined by weighing. Finally, concentrated cytochrome *c*-550 was added, immediately followed by mixing and measurement of the absorbance increase (A_t) at 550 nm as a function of time (*t*). Under these conditions, MADH and amicyanin are fully reduced at the beginning of the experiment and do not contribute to the absorbance at 550 nm while reduced cytochrome *c*-550 has an absorbance maximum at this wavelength. Afterwards, the sample was fully reduced with solid dithionite to obtain A_{∞} . The initial reaction rate v_i was obtained by determining the initial slope of the A_t versus *t* plot. The steady state reduction rate constant (k_{obs}) was derived from the slope of a plot of $\ln\{A_{\infty} - A_t\}$ versus *t*.

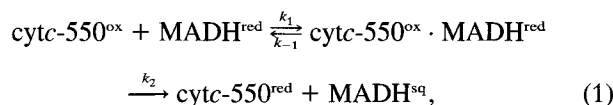
Cyclic voltammetry

Cyclic voltammetry was performed in a 400- μl standard electrochemical cell utilising an edge-plane graphite working electrode, a platinum gauze counter electrode and a saturated calomel reference electrode [35]. The protein concentration was 0.1 mM in 50 mM Hepes/NaOH, pH 8.1 (*I* = 40 mM). The ionic strength was adjusted with concentrated NaCl. Oxygen was removed from the working compartment by passing humidified oxygen-free argon through the sealed cell. Voltammograms were obtained, at room temperature, by cycling at 50–450 mV, with the use of a computer-controlled potentiostat (Oxsys Ltd.). All the potentials reported in this study are with respect to the normal hydrogen electrode.

RESULTS

Steady state reduction of cytochrome *c*-550 by MADH

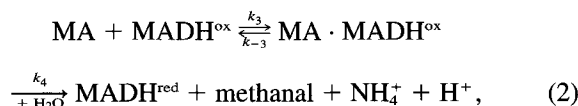
To describe the reduction of oxidized cytochrome *c*-550 by reduced MADH a simple two-step reaction model is used:



where cytc-550 is cytochrome *c*-550 and MADH^{sq} is the semiquinone form of MADH. MADH^{sq} can be oxidized further to MADH^{ox} by another equivalent of cytochrome *c*-550. No distinction is made between the first and the second oxidation reaction of MADH in this study.

The second backward reaction (k_{-2}) is neglected; the second equilibrium lies firmly to the right because of the difference in midpoint potential between MADH (estimated to be 100 mV on the basis of homology [36, 37]) and cytochrome *c*-550 (241 ± 2 mV at pH 8.1, see below).

To observe steady-state reduction it is necessary that [cytochrome *c*-550] \gg [MADH] and that [MADH^{red}] is constant. MADH^{ox} is reduced back as follows:



where MA represents methylamine.

In the experiments described in this study, the [methylamine] was 10 mM while [MADH] is up to 250 nM. Under this saturating condition [3], k_4 is the limiting factor in the back-reduction of MADH^{ox} . This rate constant is approximately 50 s^{-1} at 20°C [3] (A. C. F. Gorren, unpublished results). Therefore, the rate calculated for the reduction of MADH^{ox} is at least 100-fold greater than the fastest oxidation rate observed under the experimental conditions used in this study. Thus:

$$[\text{MADH}]_t \approx [\text{MADH}^{\text{red}}] + [\text{cytc-550}^{\text{ox}} \cdot \text{MADH}^{\text{red}}], \quad (3)$$

where $[\text{MADH}]_t$ is the total concentration of MADH. Under these conditions {[cytochrome *c*-550] \gg [MADH]_t and Eqn. (3)}, reaction 1 can be described with Michaelis-Menten kinetics as follows:

$$v = \frac{k_2 [\text{MADH}]_t [\text{cytc} - 550^{\text{ox}}]}{K_m + [\text{cytc} - 550^{\text{ox}}]}, \quad (4a)$$

$$K_m \equiv \frac{k_2 + k_{-1}}{k_1}, \quad (4b)$$

where v is the steady-state reduction rate of cytochrome *c*-550^{ox}, determined by the absorbance increase at 550 nm, and K_m is the Michaelis-Menten constant.

Fig. 2 shows a plot of the initial v (v_i) as a function of the initial [cytochrome *c*-550^{ox}] (open circles). The data have been fitted using Eqn (4a) for $K_m = 42 \pm 3 \mu\text{M}$ and $k_2 = 2.3 \pm 0.2 \text{ s}^{-1}$ (Fig. 2).

When [cytochrome *c*-550^{ox}] $\ll K_m$ Eqn (4) simplifies to:

$$v = \frac{k_2}{K_m} [\text{MADH}]_t [\text{cytc-550}^{\text{ox}}] \quad (5)$$

and thus $v \propto$ [cytochrome *c*-550^{ox}]. The straight solid line in Fig. 2 indicates that this simplification is valid up to [cytochrome *c*-550^{ox}] = 8 μM . This is confirmed by the logarithm

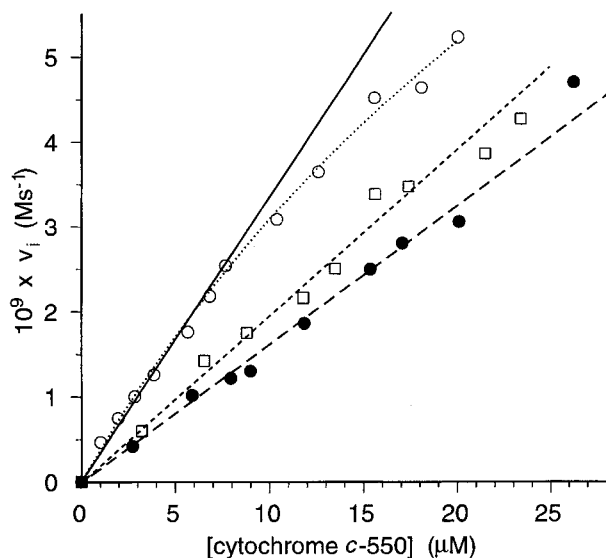


Fig. 2. Reduction of cytochrome *c*-550 by MADH. The initial velocity (v_i) of the reduction is plotted against the concentration of cytochrome *c*-550. Wild-type cytochrome *c*-550 at $I = 27$ mM (\circ); $[\text{MADH}]_i = 7$ nM; best fit of Eqn (4) to these data points with $K_m = 42 \pm 3$ μM and $k_2 = 2.3 \pm 0.2$ s^{-1} (.....); best linear fit to the data points < 5 μM (—). Wild-type cytochrome *c*-550 at $I = 0.42$ M (\bullet); $[\text{MADH}]_i = 76$ nM; best linear fit to these datapoints (—). [K14Q]cytochrome *c*-550 at $I = 27$ mM (\square); $[\text{MADH}]_i = 90$ nM; best linear fit to these datapoints (- - - -). [Methylamine] = 10 mM in all experiments.

mic behaviour of the absorbance at 550 nm in a 8.1 μM sample, as shown in Fig. 3. Fig. 3A shows the observed absorbance (A_t) and Fig. 3B shows $\ln(A_\infty - A_t)$ versus time. A_∞ is the absorbance of the fully reduced sample. The slope of the straight line is $-k_{\text{obs}}$. According to Eqn (5)

$$k_{\text{obs}} = \frac{k_2}{K_m} [\text{MADH}]_i \quad (6)$$

In Fig. 4, k_{obs} is plotted as a function of $[\text{MADH}]_i$ for wild-type and [K14Q]cytochrome *c*-550, showing a linear correlation. The slope $k_{\text{MADH}} (= k_2/K_m)$ is the steady-state reduction rate constant.

The single-charge mutation [K14Q]cytochrome *c*-550 has a large effect: k_{MADH} is 20-fold lower for the mutant (Table 1). The reduction of [K14E]cytochrome *c*-550 is even slower, approximately another 25-fold decrease, although the rates were so slow that it proved difficult to obtain reliable results. The reaction between MADH and [K14E]cytochrome *c*-550 was therefore not studied any further.

Since

$$k_{\text{MADH}} = \frac{k_2}{K_m} = \frac{k_2 k_1}{k_2 + k_{-1}} \quad (7)$$

the decrease in k_{MADH} can be caused by a decrease in k_2 or k_1 or an increase in k_{-1} . The changes in k_1 and k_{-1} would both result in a lower association constant K_a (k_1/k_{-1}). Obviously, k_2 depends on the driving force ΔG , which in its turn is dependent on the midpoint potentials of MADH and cytochrome *c*-550. The midpoint potentials of wild-type and mutant cytochrome *c*-550 were determined with cyclic voltammetry. Fig. 5 shows a representative voltammogram of cytochrome *c*-550. Although cytochrome *c*-550 has a net negative charge at pH 8.1 ($pI = 4.6$ [38]) it gives an excellent re-

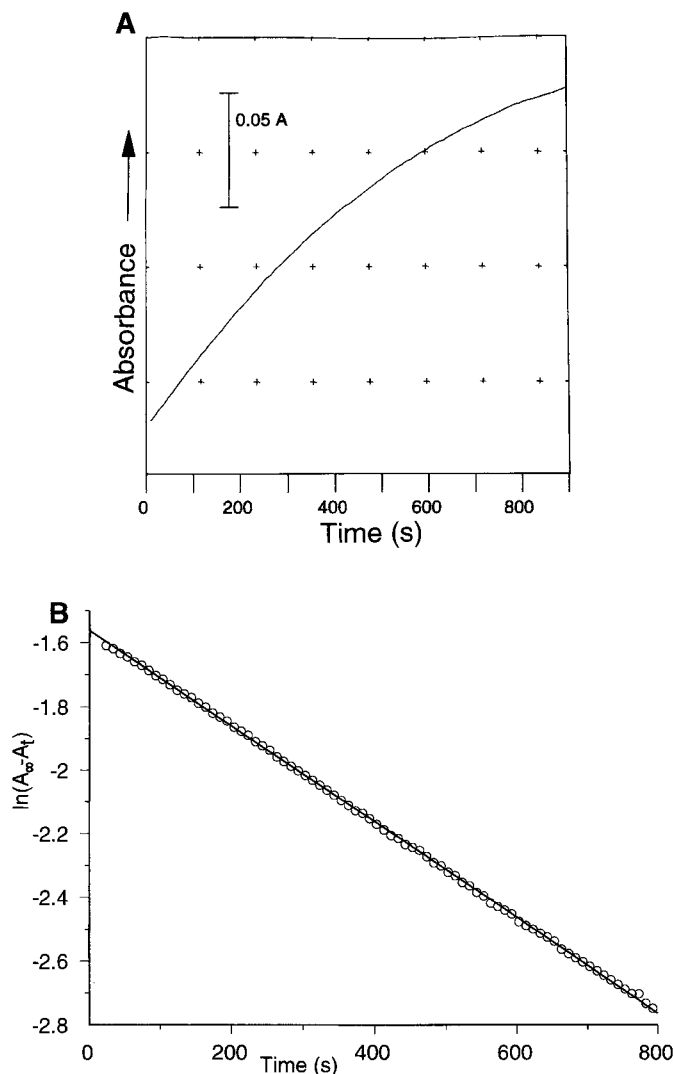


Fig. 3. Reduction of wild-type cytochrome *c*-550 by MADH. The absorbance (A_t) at 550 nm (A) and $\ln(A_\infty - A_t)$ (B) are plotted against time. [Cytochrome *c*-550] = 8.1 μM , $[\text{MADH}]_i = 31$ nM, [methylamine] = 10 mM, $I = 27$ mM. In B, the best linear fit to the data points with $k_{\text{obs}} = 1.50 \times 10^{-3}$ s^{-1} is shown.

sponse with an edge-plane graphite electrode, suggesting that a positive interaction site on the protein surface is utilised.

The midpoint potential of wild-type cytochrome *c*-550 is 241 ± 2 mV which compares well with the potentiometrically determined value of 245 ± 5 mV [38]. The mutations Lys14 \rightarrow Gln and Lys14 \rightarrow Glu have only small effects on the midpoint potential: $E^0 = 243 \pm 2$ mV ([K14Q]cytochrome *c*-550) and 249 ± 4 mV ([K14E]cytochrome *c*-550). Since these values are slightly higher than the values of the wild type, thus increasing the driving force, these changes in the midpoint potentials cannot explain the differences in k_{MADH} between wild-type and mutants.

Furthermore, a plot of v_i versus the concentration of [K14Q]cytochrome *c*-550^{ox} indicates that K_m has increased (Fig. 2, squares) since Eqn (5) applies up to higher cytochrome *c*-550 concentrations than for wild-type cytochrome *c*-550 (Fig. 2). Since k_{MADH} has decreased, this K_m increase must be caused by a decrease in K_a [either an increase of k_{-1} or a decrease of k_1 , see Eqn (7)]. Therefore, a decrease in the affinity of cytochrome *c*-550 for MADH is the major cause for the low k_{MADH} values of the mutants.

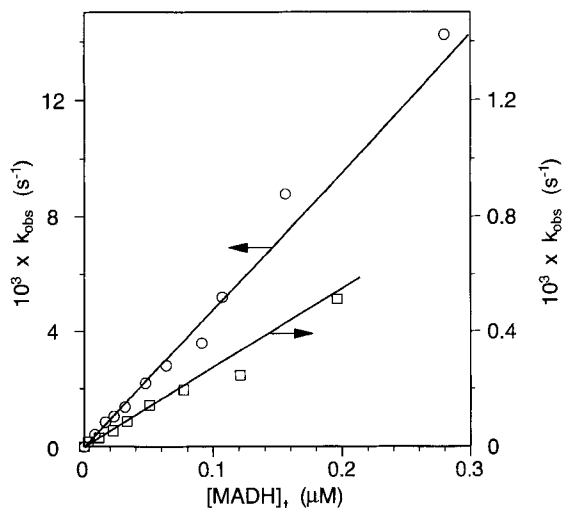


Fig. 4. Reduction of wild-type and [K14Q]cytochrome *c*-550 by MADH. The k_{obs} [see Eqn (6)] is plotted against the total concentration of MADH. [Methylamine] = 10 mM, $I = 27$ mM. \circ , left axis: wild-type cytochrome *c*-550 (5–7 μM); \square , right axis: [K14Q]cytochrome *c*-550 (7–9 μM). The best linear fits to the data points with k_{MADH} (wild type) = $52 \pm 5 \times 10^3$ and k_{MADH} ([K14Q]cytochrome *c*-550) = $2.5 \pm 0.3 \times 10^3$ $\text{M}^{-1} \text{s}^{-1}$ are shown (—).

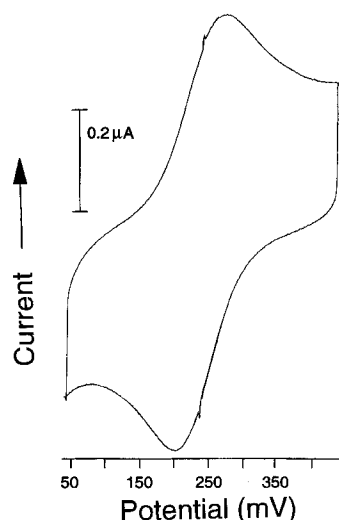


Fig. 5. Cyclic voltammogram of wild-type cytochrome *c*-550. [Cytochrome *c*-550] = 0.1 mM in 50 mM Hepes/NaOH, pH 8.1; scan speed 5 mV/s. The small spikes around 240 mV are system artefacts.

Ionic strength effects on k_{MADH}

Since the removal of a single charge has such a large effect on k_{MADH} , it was considered to be of interest to study the ionic-strength dependence of k_{MADH} for wild-type and [K14Q]cytochrome *c*-550 (Fig. 6). It is clear that the ionic-strength dependence of k_{MADH} is biphasic; while strongly decreasing towards high values of I , k_{MADH} is constant (wild type) or even increasing ([K14Q]cytochrome *c*-550) at low I . This biphasic behaviour suggests that both k_2 and K_a change with I . It also indicates that k_2 cannot be much larger than k_{-1} otherwise k_{MADH} would only depend on the rate of one reaction, the association of cytochrome *c*-550 with MADH [$k_{\text{MADH}} = k_1$, see Eqn (7)] and the curve would be monophasic.

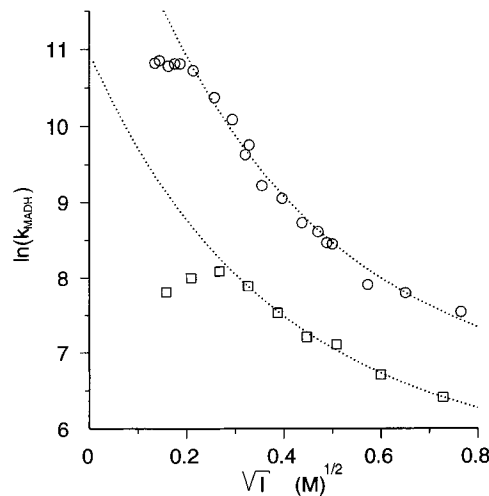


Fig. 6. Ionic-strength dependence of k_{MADH} for wild-type and [K14Q]cytochrome *c*-550. Wild-type cytochrome *c*-550 (\circ); [K14Q]cytochrome *c*-550 (\square). The best fits of Eqn (9) to the data points with $I^{1/2} > 0.3$ are shown (·····); $r = 0.8$ nm, $n = 8.8$, $k_{\infty} = 550$ $\text{M}^{-1} \text{s}^{-1}$ (wild type) and $r = 0.8$ nm, $n = 6.1$, $k_{\infty} = 258$ $\text{M}^{-1} \text{s}^{-1}$ ([K14Q]cytochrome *c*-550). [MADH] $_t$ = 23–34 nM (wild type) and 33–48 nM ([K14Q]cytochrome *c*-550); [cytochrome *c*-550] = 7–8 μM (wild type) and 5–7 μM ([K14Q]cytochrome *c*-550); [methylamine] = 10 mM.

In Fig. 2, a plot is presented of v_i versus wild-type cytochrome *c*-550 at 0.42 mM ionic strength (solid circles), showing that K_m has increased compared to the reaction at low ionic strength (although it does not allow determination of K_m and k_2 values). Thus, like the decrease observed for [K14Q]cytochrome *c*-550, the ionic-strength-dependent decrease in k_{MADH} is due to a lower affinity between cytochrome *c*-550 and MADH. Smith et al. [39] have derived an expression describing the I dependence of the rate constant (k) for reactions where the association of two proteins is rate limiting:

$$\ln(k/k_{\infty}) = C \sum_i \frac{\exp\{\kappa(a - r_i)\}}{(1 + \kappa a)r_i} \quad (8)$$

In this relationship, k_{∞} is k at infinite I , $C = 0.7057$ nm (at 302 K), $a = 0.17$ nm, the effective radius of amino and carboxylate groups (assumed to be responsible for the electrostatic interactions), r_i is the distance between such a charge pair and $\kappa = 3.27$ $I^{1/2}$ nm $^{-1}$ (at 302 K). The summation runs over all charges i with a total of n . An important assumption is that each of the n charges only interacts with one opposite charge. The strength of the interaction then depends on r_i . This allows for the single summation of all these charge interactions. As indicated by Smith et al. [39] this is normally only true for pairs of proteins that have evolved a set of complementary charges. The r_i for every pair should be determined separately to enable calculation of the curve. The authors were able to do so using preparations of cytochrome *c* modified at single lysine residues. However, often Eqn (8) is simplified to Eqn (9) [40–43]:

$$\ln(k/k_{\infty}) = C \frac{n \exp\{\kappa(a - r)\}}{(1 + \kappa a)r} \quad (9)$$

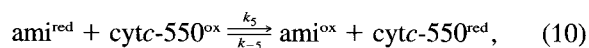
An equation very similar to Eqn (9) has also been derived by Caffrey et al. [32], based on a slightly different concept. In Eqn (9), r is an average over the r_i values. Theoretically,

Eqn (8) transforms into Eqn (9) only if all r_i values are identical. However, Eqn (9) still gives a good fit to ionic-strength dependencies, probably because fitting of three parameters (n , r and k_{∞}) allows sufficient freedom to obtain a good fit on any data set. Therefore, fits with Eqn (9) should only be interpreted in a qualitative manner. Low r values ($r < 0.4$ nm) indicate that strong, complementary interactions dominate the electrostatic interaction in the complex. The number n then gives a reasonable estimate of the number of charge pairs involved. In the case of the MADH/cytochrome *c*-550 complex the data are best fitted with high r values ($r \geq 0.8$ nm), as shown in Fig. 6, which suggests that specific complementary interactions do not play a major role.

According to Eqn (8), $\ln(k/k_{\infty})^{\text{wild type}} - \ln(k/k_{\infty})^{\text{K14Q}}$ gives the contribution of Lys14 to the ionic-strength dependence of k_{MADH} , assuming that the mutation has only affected the charge of residue 14. The difference of both curves in Fig. 6 was calculated and fitted with Eqn (8) with $n = 1$ (data not shown). This gives $r_{\text{K14}} = 0.31$ nm, which is much lower than the average of $r \approx 0.8$ nm; according to this analysis Lys14 is in close contact with negative charge(s).

Steady-state reduction of cytochrome *c*-550 by amicyanin

To establish the effects of the mutations Lys14→Gln and Lys14→Glu on the interaction between cytochrome *c*-550 and amicyanin, the steady-state reduction rate constant k_{ami} was determined for wild-type and mutant cytochrome *c*-550. In reaction 10 the overall reactions are given:



where ami is amicyanin.

For a steady-state reduction amicyanin^{ox} must be reduced back. Since ΔE° between amicyanin and cytochrome *c*-550 is small (19 mV), the backward reaction (k_{-5}) can only be neglected if the back reduction is very quick and thus [amicyanin^{ox}] is negligible. Then pseudo-first-order kinetics apply with the total amicyanin concentration, $[\text{amicyanin}]_t \approx [\text{amicyanin}^{\text{red}}]$ and $k_{\text{ami}} = k_5$:

$$v = k_{\text{ami}} [\text{ami}]_t [\text{cytc-550}]. \quad (11)$$

For this reason, methylamine and MADH were added to the reaction mixture. Since amicyanin is reduced at a high rate by MADH ($2 \times 10^7 \text{ M}^{-1} \text{ s}^{-1}$ at 20°C, pH 8; A. C. F. Gorren, unpublished results) the inequality $[\text{amicyanin}^{\text{red}}]/[\text{amicyanin}^{\text{ox}}] > 10$ is valid even for the fastest reaction of amicyanin with cytochrome *c*-550.

However, MADH^{red} can also reduce cytc^{ox} (reaction 1). As shown above, this is also a pseudo-first-order reaction. Thus, for the overall cytochrome *c*-550 reduction:

$$v = \{k_{\text{ami}}[\text{ami}]_t + k_{\text{MADH}}[\text{MADH}]_t\} [\text{cytc-550}^{\text{ox}}], \quad (12a)$$

$$k_{\text{obs}} = k_{\text{ami}}[\text{ami}]_t + k_{\text{MADH}}[\text{MADH}]_t. \quad (12b)$$

In Fig. 7, k_{obs} is plotted versus $[\text{amicyanin}]_t$ for wild-type cytochrome *c*-550 at low ionic strength. At $[\text{amicyanin}]_t > 2 \mu\text{M}$, k_{obs} starts to deviate from linear behaviour, probably because the association of amicyanin and cytochrome *c*-550 is no longer the sole rate-limiting reaction and the concentration of amicyanin/cytochrome *c*-550 complex becomes significant. For this reason $[\text{amicyanin}]_t$ was kept at $\leq 1 \mu\text{M}$ in further experiments. Fig. 8 shows plots of $k_{\text{obs}}/[\text{MADH}]_t$ versus $[\text{amicyanin}]_t/[\text{MADH}]_t$ for wild-type cytochrome *c*-550 at low and high ionic strength. In these plots,

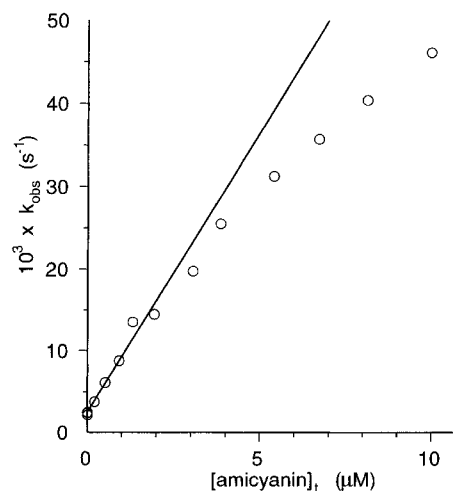


Fig. 7. Reduction of wild-type cytochrome *c*-550 by amicyanin and MADH. k_{obs} [Eqn (12b)] is plotted against the total concentration of amicyanin. [Cytochrome *c*-550] = 3–4 μM , [MADH]_t = 45 nM, [methylamine] = 10 mM, $I = 27$ mM. The best linear fit to the data points $< 2 \mu\text{M}$ is shown (—).

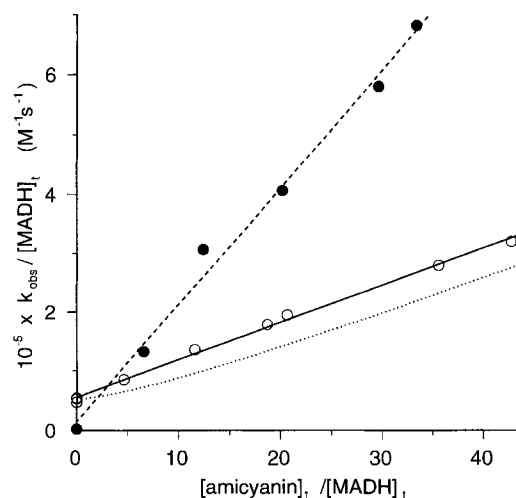


Fig. 8. Reduction of wild-type cytochrome *c*-550 by amicyanin and MADH at low and high ionic strength. $k_{\text{obs}}/[\text{MADH}]_t$ [Eqn (12b)] is plotted against the total-concentration ratio of amicyanin and MADH. [Cytochrome *c*-550] = 3–4 μM , [MADH]_t = 20 or 45 nM ($I = 27$ mM) and 29 nM ($I = 0.41$ M), [methylamine] = 10 mM. $I = 27$ mM (○); $I = 0.41$ M (●). Best linear fit to data points with $I = 27$ mM (—); best linear fit to data points with $I = 0.41$ M (---); the predicted behaviour of $k_{\text{obs}}/[\text{MADH}]_t$ on the basis of Eqn (14a) with $k_{\text{ami}} = 6.4 \times 10^3$, $k_5 = 2.6 \times 10^4$, $k_{\text{as}} = 2.0 \times 10^3 \text{ M}^{-1} \text{ s}^{-1}$, $[s]_t = 90$ nM and $K_d = 0.5 \mu\text{M}$ (see text) is shown (.....).

the slope equals k_{ami} , while the intercept is k_{MADH} [see Eqn (12b)]. Table 1 summarizes the steady-state rate constants of the reduction of wild-type and mutant cytochrome *c*-550 by amicyanin at low (27 mM) and high (0.42 M) ionic strength. The charge mutants show an increased reaction rate (wild type $< [\text{k14Q}]$ cytochrome *c*-550 $< [\text{k14E}]$ cytochrome *c*-550). The values at high I are approximately threefold higher than at low I . The salt and mutation effects are independent.

Table 1. Steady-state rate constants of the reduction of cytochrome *c*-550 by MADH and amicyanin. The rate constants have been determined at 302 K in 20 mM Hepes/NaOH, pH 8.2, +10 mM methylamine without ($I = 27$ mM) or with 0.39 M KCl ($I = 0.42$ M). n.d., not determined.

Cytochrome <i>c</i> -550	Rate constant			
	k_{MADH}		k_{ami}	
	$I = 27$ mM	$I = 0.42$ M	$I = 27$ mM	$I = 0.42$ M
	$\text{M}^{-1} \text{s}^{-1} \times 10^{-3}$			
Wild type	52 ± 5	2.3 ± 0.2	6.4 ± 0.4	20 ± 2
[K14Q] cytc-550	2.5 ± 0.3	0.7 ± 0.1	8.6 ± 0.6	28 ± 2
[K14E] cytc-550	< 0.1	n.d.	11.9 ± 0.8	32 ± 2

Complex formation between amicyanin and MADH

Evidence exists that amicyanin and MADH from *P. denitrificans*, which is related to *T. versutus*, can associate to form a complex [14, 15]. From the experiments described above, it is unclear whether complex formation takes place between amicyanin and MADH from *T. versutus* with the concentrations used (30 nM MADH, 0–1 μM amicyanin). Several possibilities exist: first, the dissociation constant for this complex is high and thus no complex formation occurs at these concentrations; secondly, the dissociation constant is very low and the MADH is complexed even at the lowest amicyanin concentration (0.2 μM); thirdly, partial complex formation takes place. In the latter case, Eqn (12b) would have to include a third reducing species, namely the $\text{MADH}^{\text{red}}/\text{amicyanin}^{\text{red}}$ complex. The MADH molecule is a functional dimer; it has two binding sites for amicyanin. The binding of amicyanin to a site can be described with a dissociation constant K_d :

$$K_d \equiv \frac{[\text{ami}][\text{s}]}{[\text{as}]}, \quad (13)$$

where $[\text{s}]$ is the concentration of unoccupied binding sites, $[\text{as}]$ is the concentration of amicyanin molecules bound to sites and $[\text{ami}]$ the concentration of unbound amicyanin. If no co-operativity exists between the binding sites, then the total concentration of sites, $[\text{s}]_t = 2 \times [\text{MADH}]_t$ and the rate constant for the reduction of a cytochrome *c*-550 by one site, k_s , is half the value of the rate constant of one MADH molecule (two sites), $k_s = 1/2 \times k_{\text{MADH}}$. Including the $\text{MADH}^{\text{red}}/\text{amicyanin}^{\text{red}}$ species transforms Eqn (12b) into:

$$k_{\text{obs}} = k_{\text{ami}} [\text{ami}]_t + k_s [\text{s}]_t + (k_{\text{as}} - k_{\text{ami}} - k_s) [\text{as}], \quad (14a)$$

with

$$[\text{ami}]_t = [\text{ami}] + [\text{as}], \quad (14b)$$

$$[\text{s}]_t = [\text{s}] + [\text{as}], \quad (14c)$$

where k_{as} is the rate constant of the reduction of cytochrome *c*-550 by the $\text{MADH}^{\text{red}}/\text{amicyanin}^{\text{red}}$ complex. When $k_{\text{as}} \neq k_s + k_{\text{ami}}$, a non-linear behaviour is predicted by Eqns 13 and 14 for the plot in Fig. 8, as indicated by the dotted line for $k_{\text{as}} < k_s + k_{\text{ami}}$ (*vide infra*).

It seems unlikely that all MADH is bound to amicyanin since the K_d would be in the 10 nM range which is rather low for an enzyme/enzyme complex. To decide between the first and third possibilities the cytochrome *c*-550 reduction system was simplified by using redox-inactive amicyanin. Then $k_{\text{ami}} = 0$ and Eqn (14a) converts to

$$k_{\text{obs}} = k_s [\text{s}]_t + (k_{\text{as}} - k_s) [\text{as}]. \quad (15)$$

Substitution of Eqns (13), (14b) and (14c) into (15) and dividing by $[\text{s}]_t$ gives the following relationships:

$$\frac{k_{\text{obs}}}{s_t} = k_s + (k_{\text{as}} - k_s) \frac{A - \sqrt{A^2 - 4s_t a_t}}{2s_t}, \quad (16a)$$

$$A = K_d + s_t + a_t, \quad (16b)$$

where $s_t = [\text{s}]_t$ and $a_t = [\text{amicyanin}]_t$. Eqn (16) can be reformulated using basic algebra as:

$$K_d = \frac{k_{\text{obs}} - k_s s_t}{k_{\text{as}} - k_s} - \frac{a_t \{k_{\text{obs}} - k_s s_t\}}{k_{\text{obs}} - k_s s_t}. \quad (17)$$

Ag^+ -amicyanin and Zn^{2+} -amicyanin were prepared as described in the Materials and Methods section, to serve as redox inactive analogues of Cu^+ -amicyanin and Cu^{2+} -amicyanin, respectively. Both metals were readily incorporated into apo-amicyanin. The products behaved as native amicyanin on a IEF gel and inhibited reconstitution with Cu ions completely. Apo-amicyanin was not used as a redox-inactive analogue in the reduction experiments since it can incorporate even traces of Cu ions and thus form redox-active amicyanin.

The reduction rate of cytochrome *c*-550 by MADH was studied in the presence of Ag^+ -amicyanin and Zn^{2+} -amicyanin as shown in Fig. 9, where $k_{\text{obs}}/[\text{s}]_t$ is plotted versus $[\text{Zn}^{2+}\text{-amicyanin}]_t$ and $[\text{Ag}^+\text{-amicyanin}]_t$. Remarkably, Zn^{2+} -amicyanin shows a strong inhibition of the reduction while Ag^+ -amicyanin hardly has any effect on the rate. All compounds used in the preparation of Ag^+ -amicyanin and Zn^{2+} -amicyanin were thoroughly removed by washing. To confirm that no inhibitors are present however, reduction reactions in the absence of amicyanin but in the presence of 20 μM Zn^{2+} , CN^- or EDTA were performed. No inhibition was observed. These results indicate that MADH binds Zn^{2+} -amicyanin much stronger than Ag^+ -amicyanin. The solid line in Fig. 9 was fitted to the data points of Zn^{2+} -amicyanin by variation of k_{as} in Eqn (16) with $k_s = 2.6 \times 10^4 \text{ M}^{-1} \text{ s}^{-1}$ and $[\text{s}]_t = 0.10 \mu\text{M}$. When $k_{\text{as}} = 2.0 \times 10^3 \text{ M}^{-1} \text{ s}^{-1}$ the best fit is obtained with $K_d = 0.5 \pm 0.1 \mu\text{M}$. The dotted line represents $k_{\text{as}} = 0 \text{ M}^{-1} \text{ s}^{-1}$ which gives $K_d = 0.8 \pm 0.3 \mu\text{M}$. This curve clearly does not fit the data as well as in the previous case. The reduction of cytochrome *c*-550^{ox} by MADH^{red} bound to Zn^{2+} -amicyanin is thus severely hindered (13-fold) although not completely prevented.

Since the electronic properties, charge and ionic radius of Zn^{2+} and Ag^+ , resemble those of Cu^{2+} and Cu^+ , respec-

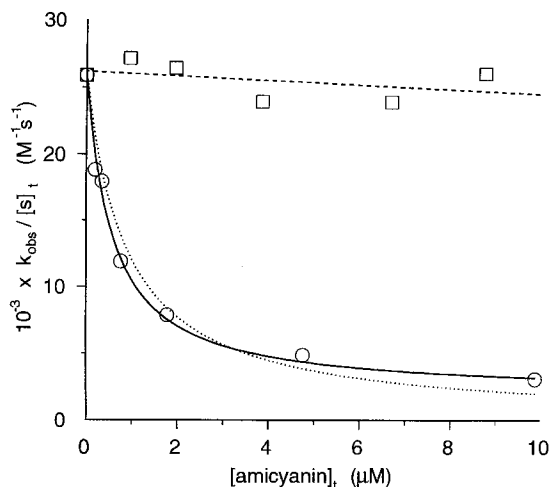


Fig. 9. Inhibition with redox-inactive amicyanin of wild-type cytochrome *c*-550 reduction by MADH. $k_{\text{obs}}/[s]_t$ [Eqn (16)] is plotted against the concentrations of Zn^{2+} -amicyanin (\circ) and Ag^+ -amicyanin (\square). [Cytochrome *c*-550] = 3–4 μM ; [MADH]_t = 50 nM (Zn^{2+} -amicyanin) and 60 nM (Ag^+ -amicyanin); [methylamine] = 10 mM; I = 27 mM. Best linear fit to the Ag^+ -amicyanin data points (---). Best fit of Eqn (16) to the Zn^{2+} -amicyanin data points with $k_{\text{as}} = 2.6 \times 10^4 \text{ M}^{-1} \text{ s}^{-1}$ and $[s]_t = 100 \text{ nM}$ (—); the optimal value of $k_{\text{as}} = 2.0 \times 10^3 \text{ M}^{-1} \text{ s}^{-1}$ gives $K_{\text{d}} = 0.5 \pm 0.1 \mu\text{M}$; best fit of Eqn (16) to the Zn^{2+} -amicyanin data points with $k_{\text{as}} = 0$ and $[s]_t = 100 \text{ nM}$, which gives $K_{\text{d}} = 0.8 \pm 0.3 \mu\text{M}$ (.....).

tively, these results suggest that MADH can form a much stronger complex with Cu^{2+} -amicyanin than with Cu^+ -amicyanin. Under the conditions used in the experiments with Cu -amicyanin, (almost) all amicyanin is present as Cu^+ -amicyanin (as discussed above). Therefore no amicyanin/MADH complexes are present, which explains the linear behaviour in Fig. 8. If Cu^+ -amicyanin would have formed a complex with MADH with the parameters found for Zn^{2+} -amicyanin/MADH ($K_{\text{d}} = 0.5 \mu\text{M}$; $k_{\text{as}} = 2.0 \times 10^3 \text{ M}^{-1} \text{ s}^{-1}$) the dotted line in Fig. 8 would have been obtained.

DISCUSSION

The steady-state rate constant of the reduction of wild-type cytochrome *c*-550 by MADH (k_{MADH}) that has been determined in this study is higher than the (non-steady state) rate constant reported by van Wielink et al. [3], $33 \pm 3 \times 10^3$ versus $1 \times 10^3 \text{ M}^{-1} \text{ s}^{-1}$, respectively, at $I = 60 \text{ mM}$. This difference may be related to the high specific activity of the MADH used in this study and to a difference in environmental conditions: a higher pH and temperature used in our experiments (pH 8.2 versus 7.0 and temperature 29°C versus 20°C).

The ionic-strength dependence of k_{MADH} is biphasic (Fig. 6). The large decrease at high I reflects an increase in K_{m} . Thus, the affinity of both proteins for each other has diminished (K_{a} is lower) due to screening of protein charges by salt ions. This suggests the presence of a charged binding site on MADH, which is expected to be negative given the ring of positive charges around the heme crevice of cytochrome *c*-550 (see Fig. 1).

If k_{MADH} values were solely dependent on the association rate of cytochrome *c*-550 with MADH (k_1) then a monotonical behaviour would be expected for the ionic-strength dependence (Fig. 6). At low I values, the data clearly deviate

from this, which is tentatively ascribed to changes in k_2 [see Eqn (7)]. The k_2 value increases with I but only over a limited range of 25–90 mM. This behaviour has been observed in other protein complexes [44–46] and is thought to indicate that the proteins in the complex need some conformational freedom to achieve optimal electron transfer. At low ionic strength, the proteins are fixed in a less productive orientation while partial screening of electrostatic forces by ions allows for rearrangement in the complex resulting in more productive orientations. This model implies the absence of permanent specific complementary charge pairs, which is in agreement with the finding that ionic-strength dependence of k_{MADH} can be fitted best with high r values [see Eqn (9)].

Mutation of Lys14 has considerable effect on the reduction rate of cytochrome *c*-550 by MADH. Removal of the positive charge (Lys14→Gln) lowers k_{MADH} 20-fold while substitution with a negative charge results in a 500-fold decrease of k_{MADH} . These changes must be ascribed to decreases in the affinity between cytochrome *c*-550 and MADH since the K_{m} is much larger for [K14Q]cytochrome *c*-550. This supports the suggestion of a negative binding site on MADH.

Lys14 plays an important role in the interaction between both proteins. The ionic-strength dependence of [K14Q]cytochrome *c*-550 is 30% lower ($1 - n_{\text{K14Q}}/n_{\text{wild type}}$ with $r = 0.8 \text{ nm}$) and $r_{\text{K14}} = 0.31 \text{ nm}$, much lower than the average of 0.8 nm. Thus, Lys14 is probably in close contact with negative groups in many or all possible orientations of cytochrome *c*-550 in the complex. It has been shown for other *c*-type cytochromes in many studies that this conserved lysine residue often, if not always, is involved in electrostatic interactions in complexes with other proteins. Clearly, this is also true for cytochrome *c*-550 from *T. versutus* [22, this study].

The midpoint potential of cytochrome *c*-550 is only slightly influenced by mutation of Lys14. Conversion to a negative charge raises E^0 8 mV. This increase is somewhat surprising since intuitively negative charge would be expected to stabilize the oxidized form relative to the reduced form, as observed for cytochrome *c* [47] and cytochrome *c*₂ [48]. NMR studies have shown that the heme environment is subtly perturbed in the Lys14 mutants [22], which can perhaps explain this phenomenon. No ionic-strength dependence is observed for E^0 in the range of 40 mM to 0.7 M (data not shown), in agreement with the finding that E^0 of *c*-type cytochromes only shows significant ionic-strength dependence at small I values [47–50].

The reduction rate by amicyanin is higher for mutant than for wild-type cytochrome *c*-550 ([K14E]cytochrome *c*-550 > [K14Q]cytochrome *c*-550 > wild type). The effects are smaller than in the case of MADH. They may partly be caused by the increase in E^0 of the mutants. The finding that the mutation effects are not masked at high I is compatible with this and suggests that the mutations have little influence on electrostatic interactions. The reduction rates increase with increasing ionic strength, although the increase is small (threefold). These effects could be due to screening of unfavourable electrostatic interactions or a decrease of E^0 of amicyanin with I . It is clear from both mutation and ionic strength effects that electrostatic interactions do not play an important role in the formation of the complex of amicyanin and cytochrome *c*-550. This is in agreement with the fact that amicyanin has no evident negative patch on its surface (contrary to plastocyanin). Therefore, the most obvious reaction site for cytochrome *c*-550 would be near His96 in anal-

ogy with azurin [51, 52]. This would give the shortest Cu-Fe distance for electron transfer and this patch has a hydrophobic nature; it is surrounded only by few charged residues.

A remarkable result from this study is that wild-type cytochrome *c*-550 is reduced eightfold quicker by MADH than by amicyanin, although amicyanin is a proposed redox partner of cytochrome *c*-550 [3]. Still, it can be expected that under physiological conditions electrons flow from MADH via amicyanin to cytochrome *c*-550 since amicyanin is reduced by MADH much faster than cytochrome *c*-550 ($10^{\text{threefold}}$). The inhibition experiments with redox-inactive amicyanin suggest a high binding affinity of MADH for substrate (Cu^{2+} -amicyanin) and low affinity for product (Cu^+ -amicyanin). Interestingly, Davidson et al. [53] have recently found that a complex of *P. denitrificans* MADH with Cu^{2+} -amicyanin has a much lower K_a compared to a complex of MADH with apo-amicyanin. Considering the fact that Cu^{2+} -amicyanin and apo-amicyanin, like Cu^{2+} -amicyanin and Cu^+ -amicyanin, have a charge difference of one on the Cu site, this result supports the findings described in this study. The difference in affinity of MADH for Cu^{2+} -amicyanin and Cu^+ -amicyanin could well contribute to the high reduction rate of amicyanin because the association rate of substrate can be high without causing product inhibition. Why Cu^{2+} -amicyanin binds better to MADH than Cu^+ -amicyanin is unclear. It has been shown that protonation of His96 of amicyanin causes loss of the ligation of the histidine residue to the Cu when amicyanin is in the reduced form, probably due to rotation of the side chain [54]. Perhaps this histidine is protonated in the amicyanin/MADH complex upon reduction of the Cu. His96 is in the middle of the contact site of amicyanin and MADH in the crystal structure of the complex and in between the Cu and the tryptophan tryptophylquinone cofactor [14]. Rotation of the histidine residue could therefore affect the stability of the complex.

It has been proposed that MADH, amicyanin and cytochrome *c*-550 of *P. denitrificans* can form a ternary complex [55]. The assumed instability of the reduced MADH/amicyanin complex is difficult to reconcile with a physiological role for such a ternary complex. It would fall apart upon reduction of amicyanin, unless the electron is very rapidly transferred from the Cu to the heme Fe.

The question arises why the reduction rate of cytochrome *c*-550 by amicyanin is so poor while the reduction of amicyanin by MADH appears to be evolutionarily optimized. It is possible that amicyanin does not normally donate electrons to cytochrome *c*-550 but to another protein. The only other soluble cytochrome found in methylamine-grown *T. versutus* is cytochrome *c*-552, which does not show any reaction with MADH or amicyanin [3]. Amicyanin may donate electrons directly to cytochrome *aa*₃. However, it is expected that cytochrome *c*-550 (which is homologous to mitochondrial cytochrome *c*) is optimized for the reaction with cytochrome *aa*₃ and will react much faster than amicyanin. Therefore, the electron transfer route from MADH via amicyanin to cytochrome *c*-550 and then to cytochrome *aa*₃ is the most probable one. It may be that cytochrome *c*-550 is not optimized for the reaction with amicyanin because amicyanin is not its usual redox partner (expression of cytochrome *c*-550 is not limited to growth on methylamine [56] and cytochrome *c*-550 could well be involved in other redox reactions) or because a fast reaction is unnecessary. The latter explanation is quite feasible since in the bacterium the concentrations of all components are as important as the rate constants in

determining the overall electron-transfer rate. Speculatively, it is proposed that under natural conditions the [methylamine] is rate limiting. The concentration of MADH^{ox} should then be as high as possible to bind large amounts of methylamine. This would explain the high induction levels of amicyanin and MADH [3] and the optimization of the reduction of amicyanin by MADH; quick regeneration of reduced MADH to the oxidized form by amicyanin would be a necessity. Amicyanin would then serve as a 'buffer' for electrons from where they can flow via cytochrome *c*-550 to cytochrome *aa*₃.

Prof. Dr J. A. Duine and Dr A. C. F. Gorren are acknowledged for their critical comments on the manuscript. Support to M.U. from NATO travel grant number CRG 900603 is gratefully acknowledged.

REFERENCES

- Vellieux, F. M. D., Frank Jzn, J., Swarte, M. B. A., Groendijk, H., Duine, J. A., Drenth, J. & Hol, W. G. J. (1986) Purification, crystallization and preliminary X-ray investigation of quinoprotein methylamine dehydrogenase from *Thiobacillus versutus*, *Eur. J. Biochem.* **154**, 383–386.
- van Houwelingen, T., Canters, G. W., Stobbelaar, G., Duine, J. A., Frank Jzn, J. & Tsugita, A. (1985) Isolation and characterization of a blue copper protein from *Thiobacillus versutus*, *Eur. J. Biochem.* **153**, 75–80.
- van Wielink, J. E., Frank Jzn, J. & Duine, J. A. (1989) in *PQQ and quinoproteins* (Jongejan, J. A. & Duine, J. A., eds) pp. 269–278, Kluwer Academic Publishers, Dordrecht.
- van Spanning, R. J. M., Wansell, C. W., Reijnders, W. N. M., Oltmann, L. F. & Stouthamer, A. H. (1990) Mutagenesis of the gene encoding amicyanin of *Paracoccus denitrificans* and the resultant effect on methylamine oxidation, *FEBS Lett.* **275**, 217–220.
- Husain, M. & Davidson, V. L. (1986) Characterization of two inducible periplasmic *c*-type cytochromes from *Paracoccus denitrificans*, *J. Biol. Chem.* **261**, 8577–8580.
- Davidson, V. L. & Kumar, M. A. (1989) Cytochrome *c*-550 mediates electron transfer from inducible periplasmic *c*-type cytochromes to the cytoplasmic membrane of *Paracoccus denitrificans*, *FEBS Lett.* **245**, 271–273.
- van Spanning, R. J. M., Wansell, C. W., Harms, N., Oltmann, L. F. & Stouthamer, A. H. (1990) Mutagenesis of the gene encoding cytochrome *c*-550 of *Paracoccus denitrificans* and analysis of the resultant physiological effects, *J. Bacteriol.* **172**, 986–996.
- van Spanning, R. J. M., Wansell, C. W., Reijnders, W. N. M., Harms, N., Ras, J., Oltmann, L. F. & Stouthamer, A. H. (1991) A method for introduction of unmarked mutations in the genome of *Paracoccus denitrificans*: construction of strains with multiple mutations in the genes encoding periplasmic cytochromes *c*-550, *c*-551i, and *c*-553i, *J. Bacteriol.* **173**, 6962–6970.
- Chandrasekar, R. & Klapper, M. H. (1986) Methylamine dehydrogenase and cytochrome *c*-552 from bacterium W3A1, *J. Biol. Chem.* **261**, 3616–3619.
- Fukumori, Y. & Yamanaka, T. (1987) The methylamine oxidizing system of *Pseudomonas* AM1 reconstituted with purified components, *J. Biochem. (Tokyo)* **101**, 441–445.
- Ubbink, M., van Kleef, M. A. G., Kleinjan, D.-J., Hoitink, C. W. G., Huitema, F., Beintema, J. J., Duine, J. A. & Canters, G. W. (1991) Cloning, sequencing and expression studies of the genes encoding amicyanin and the β -subunit of methylamine dehydrogenase from *Thiobacillus versutus*, *Eur. J. Biochem.* **202**, 1003–1012.
- Vellieux, F. M. D., Huitema, F., Groendijk, H., Kalk, K. H., Frank Jzn, J., Jongejan, J. A., Duine, J. A., Petratos, K., Drenth, J. & Hol, W. G. J. (1989) Structure of quinoprotein

- methylamine dehydrogenase at 2.25 Å resolution, *EMBO J.* 8, 2171–2178.
13. Durley, R., Chen, L., Lim, L. W., Mathews, F. S. & Davidson, V. L. (1993) Crystal structure analysis of amicyanin and apo-amicyanin from *Paracoccus denitrificans* at 2.0 Å and 1.8 Å resolution, *Protein Sci.* 2, 739–752.
 14. Chen, L., Durley, R., Poliks, B. J., Hamada, K., Chen, Z., Mathews, F. S., Davidson, V. L., Satow, Y., Huizinga, E. & Vellieux, F. M. D. (1992) Crystal structure of an electron transfer complex between methylamine dehydrogenase and amicyanin, *Biochemistry* 31, 4959–4964.
 15. Gray, K. A., Davidson, V. L. & Knaff, D. B. (1988) Complex formation between methylamine dehydrogenase and amicyanin from *Paracoccus denitrificans*, *J. Biol. Chem.* 263, 13987–13990.
 16. Kalverda, A. P., Lommen, A., Wijmenga, S., Hilbers, C. W. & Canters, G. W. (1991) Three dimensional structure determination of amicyanin by NMR and MD simulations, *J. Inorg. Biochem.* 43, 171.
 17. McIntire, W. S., Wemmer, D. E., Chistoserdov, A. & Lidstrom, M. E. (1991) A new cofactor in a prokaryotic enzyme: tryptophan tryptophylquinone as the redox prosthetic group in methylamine dehydrogenase, *Science* 252, 817–824.
 18. Chistoserdov, A. Y., Boyd, J., Mathews, F. S. & Lidstrom, M. E. (1992) The genetic organization of the *mau* gene cluster of the facultative autotroph *Paracoccus denitrificans*, *Biochem. Biophys. Res. Commun.* 184, 1226–1234.
 19. Chistoserdov, A. Y., Tsygankov, Y. D. & Lidstrom, M. E. (1991) Genetic organization of methylamine utilization genes from *Methylobacterium extroquens* AM1, *J. Bacteriol.* 173, 5901–5908.
 20. Huitema, F., Van Beeumen, J., Van Driessche, G., Duine, J. A. & Canters, G. W. (1993) Cloning and sequencing of the gene coding for the large subunit of methylamine dehydrogenase from *Thiobacillus versutus*, *J. Bacteriol.* 175, 6254–6259.
 21. Ubbink, M., Van Beeumen, J. & Canters, G. W. (1992) Cytochrome *c*₅₅₀ from *Thiobacillus versutus*: cloning, expression in *Escherichia coli*, and purification of the heterologous holo-protein, *J. Bacteriol.* 174, 3707–3714.
 22. Ubbink, M. & Canters, G. W. (1993) Mutagenesis of the conserved Lys14 of cytochrome *c*-550 from *Thiobacillus versutus* affects the protein structure and the electron self-exchange rate, *Biochemistry* 32, 13893–13901.
 23. Kornblatt, J. A., Theodorakis, J., Hui Bon Hoa, G. & Margoliash, E. (1992) Cytochrome *c* and cytochrome *c* oxidase interactions: the effects of ionic strength and hydrostatic pressure studied with site-specific modifications of cytochrome *c*, *Biochem. Cell Biol.* 70, 539–547.
 24. Hahm, S., Durham, B. & Millett, F. (1992) Photoinduced electron transfer between cytochrome *c* peroxidase and horse cytochrome *c* labeled at specific lysines with (dicarboxy-bipyridine)(bisbipyridine)ruthenium(II), *Biochemistry* 31, 3472–3477.
 25. Pelletier, H. & Kraut, J. (1992) Crystal structure of a complex between electron transfer partners, cytochrome *c* peroxidase and cytochrome *c*, *Science* 258, 1748–1755.
 26. Roberts, V. A., Freeman, H. C., Olson, A. J., Tainer, J. A. & Getzoff, E. D. (1991) Electrostatic orientation of the electron-transfer complex between plastocyanin and cytochrome *c*, *J. Biol. Chem.* 266, 13431–13441.
 27. Moore, G. R. & Pettigrew, G. W. (1990) *Cytochromes c, evolutionary, structural and physicochemical aspects*, Springer-Verlag, Berlin.
 28. Pettigrew, G. W. & Moore, G. R. (1987) *Cytochromes c, biological aspects*, Springer-Verlag, Berlin.
 29. Rush, J. D., Koppenol, W. H., Garber, E. A. E. & Margoliash, E. (1988) Conformational stability of ferrocyanochrome *c*, *J. Biol. Chem.* 263, 7514–7520.
 30. Concar, D. W., Hill, H. A. O., Moore, G. R., Whitford, D. & Williams, R. J. P. (1986) The modulation of cytochrome *c* electron self-exchange by site-specific chemical modification and anion binding, *FEBS Lett.* 206, 15–19.
 31. Bosshard, H. R., Wynn, R. M. & Knaff, D. B. (1987) Binding site on *Rhodospirillum rubrum* cytochrome *c*₂ for the *Rhodospirillum rubrum* cytochrome *bc*₁ complex, *Biochemistry* 26, 7688–7693.
 32. Caffrey, M. S., Bartsch, R. G. & Cusanovich, M. A. (1992) Study of the cytochrome *c*₂-reaction center interaction by site-directed mutagenesis, *J. Biol. Chem.* 267, 6317–6321.
 33. van de Kamp, M., Hali, F. C., Rosato, N., Finazzi Agro, A. & Canters, G. W. (1990) Purification and characterization of a non-reconstitutable azurin, obtained by heterologous expression of the *Pseudomonas aeruginosa* *azu* gene in *Escherichia coli*, *Biochim. Biophys. Acta* 1019, 283–292.
 34. van Wielink, J. E., Frank, J. & Duine, J. A. (1990) Methylamine dehydrogenase from *Thiobacillus versutus*, *Methods Enzymol.* 188, 235–241.
 35. Armstrong, F. A., Hill, H. A. O. & Walton, N. J. (1986) Reactions of electron-transfer proteins at electrodes, *Q. Rev. Biophys.* 18, 261–322.
 36. Burrows, A. L., Hill, H. A. O., Leese, T. A., McIntire, W. S., Nakayama, H. & Sanghera, G. S. (1991) Direct electrochemistry of the enzyme, methylamine dehydrogenase, from bacterium W3A1, *Eur. J. Biochem.* 199, 73–78.
 37. Husain, M., Davidson, V. L., Gray, K. A. & Knaff, D. B. (1987) Redox properties of the quinoprotein methylamine dehydrogenase from *Paracoccus denitrificans*, *Biochemistry* 26, 4139–4143.
 38. Lommen, A., Ratsma, A., Bijlsma, N., Canters, G. W., van Wielink, J. E., Frank, J. & Van Beeumen, J. (1990) Isolation and characterization of cytochrome *c*₅₅₀ from the methylamine-oxidizing electron-transport chain of *Thiobacillus versutus*, *Eur. J. Biochem.* 192, 653–661.
 39. Smith, H. T., Ahmed, A. J. & Millet, F. (1981) Electrostatic interaction of cytochrome *c* with cytochrome *c*₁ and cytochrome oxidase, *J. Biol. Chem.* 256, 4984–4990.
 40. Stonehuerner, J., Williams, J. B. & Millett, F. (1979) Interaction between cytochrome *c* and cytochrome *b*_s, *Biochemistry* 18, 5422–5427.
 41. Hall, J., Zha, X., Durham, B., O'Brien, P., Vieira, B., Davis, D., Okamura, M. & Millett, F. (1987) Reaction of cytochrome *c* and *c*₂ with the *Rhodobacter sphaeroides* reaction center involves the heme crevice domain, *Biochemistry* 26, 4494–4500.
 42. Knaff, D. B., Willie, A., Long, J. E., Kriauciunas, A., Durham, B. & Millett, F. (1991) Reaction of cytochrome *c*₂ with photosynthetic reaction centers from *Rhodospseudomonas viridis*, *Biochemistry* 30, 1303–1310.
 43. Guner, S., Willie, A., Millett, F., Caffrey, M. S., Cusanovich, M. A., Robertson, D. E. & Knaff, D. B. (1993) The interaction between cytochrome *c*₂ and the cytochrome *bc*₁ complex in the photosynthetic purple bacteria *Rhodobacter capsulatus* and *Rhodospseudomonas viridis*, *Biochemistry* 32, 4793–4800.
 44. Meyer, T. E., Zhao, Z. G., Cusanovich, M. A. & Tollin, G. (1993) Transient kinetics of electron transfer from a variety of *c*-type cytochromes to plastocyanin, *Biochemistry* 32, 4552–4559.
 45. Hervas, M., De La Rosa, M. A. & Tollin, G. (1992) A comparative laser-flash absorbance spectroscopy study of algal plastocyanin and cytochrome *c*-552 photooxidation by photosystem I particles from spinach, *Eur. J. Biochem.* 203, 115–120.
 46. Hazzard, J. T., Rong, S.-Y. & Tollin, G. (1991) Ionic-strength dependence of the kinetics of electron transfer from bovine mitochondrial cytochrome *c* to bovine cytochrome *c* oxidase, *Biochemistry* 30, 213–222.
 47. Aviram, I., Myer, Y. P. & Schejter, A. (1981) Stepwise modification of the electrostatic charge of cytochrome *c*, *J. Biol. Chem.* 256, 5540–5544.
 48. Caffrey, M. S. & Cusanovich, M. A. (1991) The effects of surface charge on the redoxpotential of cytochrome *c*₂ from the purple phototrophic bacterium *Rhodobacter capsulatus*, *Arch. Biochem. Biophys.* 285, 227–230.

49. Goldkorn, T. & Schejter, A. (1976) The redox potential of cytochrome *c*-552 from *Euglena gracilis*: a thermodynamic study, *Arch. Biochem. Biophys.* **177**, 39–45.
50. Margalit, R. & Schejter, A. (1973) Cytochrome *c*: a thermodynamic study of the relationships among oxidation state, ion-binding and structural parameters, *Eur. J. Biochem.* **32**, 492–499.
51. van de Kamp, M., Silvestrini, M. C., Brunori, M., Van Beeumen, J., Hali, F. C. & Canters, G. W. (1990) Involvement of the hydrophobic patch of azurin in electron transfer reactions with cytochrome *c*-551 and nitrite reductase, *Eur. J. Biochem.* **194**, 109–118.
52. van de Kamp, M., Floris, R., Hali, F. C. & Canters, G. W. (1990) Site-directed mutagenesis reveals that the hydrophobic patch of azurin mediates electron transfer, *J. Am. Chem. Soc.* **112**, 907–908.
53. Davidson, V. L., Graichen, M. E. & Jones, L. H. (1993) Binding constants for a physiological electron-transfer protein complex between methylamine dehydrogenase and amicyanin. Effect of ionic strength and bound copper on binding, *Biochim. Biophys. Acta* **1144**, 39–45.
54. Lommen, A. & Canters, G. W. (1990) pH-dependent redox-activity and fluxionality of the copper site in amicyanin from *T. versutus* as studied by 300 and 600 MHz ¹H-NMR, *J. Biol. Chem.* **265**, 2768–2774.
55. Chen, L., Mathews, F. S., Davidson, V. L., Tegoni, M., Rivetti, C. & Rossi, G. L. (1993) Preliminary crystal structure studies of a ternary electron transfer complex between a quinoprotein, a blue copper protein, and a *c*-type cytochrome, *Protein Sci.* **2**, 147–154.
56. Lu, W.-P. & Kelly, D. P. (1984) Purification and characterization of two essential cytochromes of the thiosulphate-oxidizing multienzyme system from *Thiobacillus A2* (*Thiobacillus versutus*), *Biochim. Biophys. Acta* **765**, 106–117.
57. Timkovich, R. & Dickerson, R. E. (1976) The structure of *Paracoccus denitrificans* cytochrome *c*₅₅₀, *J. Biol. Chem.* **251**, 4033–4046.
58. Kraulis, P. J. (1991) MOLSCRIPT: a program to produce both detailed and schematic plots of protein structures, *J. Appl. Cryst.* **24**, 946–950.